HIGH SPEED FRACTURE IN POLYMERS AND COMPOSITES

J.G. WILLIAMS
Imperial College of Science, Technology and Medicine
Mechanical Engineering Department,
London, SW7 2BX, UK

ABSTRACT

An analysis of dynamic crack growth in loaded strips and beams is described which employs the static displacement fields to compute the kinetic energy. This approximation yields steady state solutions which are close to the crack growth histories observed experimentally. However such steady states require finite crack velocities at initiation from finite crack length and this cannot be achieved. There are thus induced oscillating variations in crack speed which can be discerned in the experiments and are described by the analysis.

KEYWORDS Dynamic, delamination, steady state, purturbations

INTRODUCTION

Characterising the toughness of composite laminates via fracture mechanics is now quite well developed [eg 1, 2]. Tests for the determination of G_{IC}, G_{IIC} and mixed mode systems have been widely studied and are reasonably well understood (some mysteries still surround mode II tests however). In most of the mode I tests delaminations are propagated in a stable manner at low speeds to determine G_{IC} as a function of crack growth, ie the $'R''$ curve. The tests are usually double cantilever beams in which,

$$G_{IC} \propto \frac{u_o^2}{a^4}$$

where u_o is the load point displacement and a is the crack, or delamination length. If G_{IC} remains constant and the specimen is loaded at a constant rate V then

$$\frac{V^2 t^2}{a^4} \propto \text{constant}$$

and the crack growth history is of the form,

$$a = A\sqrt{t}$$

where A is a constant and $\dot{a} = \frac{A}{2\sqrt{t}}$ ie the crack slows down during propagation.

In general rather low loading speeds and hence low crack speeds are used, but it has been recognised that many delaminations arise as impact damage and are thus rapid and that such higher speeds would be more appropriate for characterisation. Experimentally such tests are demanding but feasible, with loading rates of up to 25 m/s possible. Measurements are quite difficult, but high speed cameras enable all the necessary information to be retrieved [3, 4]. However there remains an underlying problem in that the usual specimens are rather slender beams and there are substantial dynamic effects. These have been studied [5, 6, 7] with a view to correcting the data as necessary, but also to understanding the behaviour of such structures when loaded rapidly. Exact solutions for such problems are rare, but it turns out that a scheme based on static displacement fields, the Berry method [8, 9], and perturbation analysis yields useful results [4,7]. These last references have explored the DCB test in detail and it will be described here, but first it is useful to look at another configuration which gives a rather simpler result.

THE AXIALLY LOADED STRIP

This simple configuration is shown in fig 1 and would be in mode II. It was analysed in some detail elsewhere [2, 10] where it was shown that the static G is given by,

$$G_s = \frac{Eh}{2}\left(\frac{u_o}{a}\right)^2 \tag{1}$$

and that the solution is the same for the torsion loaded strip [10] for which E is replaced by $\frac{1}{3}\left(\frac{b}{d}\right)^2\mu$, μ is the shear modulus and d is the distance between the load points and for the shear beam [10] in which is E is replaced by $\frac{2}{3}\mu$. The displacement distribution in the strip is,

$$u = u_o\left(1-\frac{x}{a}\right) \tag{2}$$

and hence for a crack speed $\dot{a}$ and when $u_o = Vt$

$$\dot{u} = V\left[1-\left(1-\frac{\dot{a}t}{a}\right)\frac{x}{a}\right] \tag{3}$$

The dynamic G is,

$$G = G_s - \frac{1}{b}\frac{dU_k}{da}$$

where U_k is the kinetic energy given by,

$$U_k = \frac{1}{2}\rho bh.\int_o^a \dot{u}^2 dx$$

ie $$U_k = \rho bha\frac{V^2}{6}\left[1+\frac{\dot{a}t}{a}+\left(\frac{\dot{a}t}{a}\right)^2\right]$$

where ρ is the density. Differentiating again we have

$$\frac{dU_k}{bda} = \frac{Eh}{6}.\left(\frac{V}{c}\right)^2\left[2+2\frac{\dot{a}t}{a}-\left(\frac{\dot{a}t}{a}\right)^2+\frac{\ddot{a}t}{\dot{a}}+2\frac{\ddot{a}t^2}{a}\right] \tag{4}$$

and $c^2 = \frac{E}{\rho}$ the wave speed.

We may use the expression for G assuming that $G = G_o$, a constant, for propagation. There are three cases of interest.

1) Initiation

For the period up to initiation $G < G_o$ with $\dot{a} = \ddot{a} = 0$ and at initiation,

$$G = G_1 = \frac{Eh}{2}.\left(\frac{Vt_o}{a_o}\right)^2 - \frac{Eh}{3}\left(\frac{V}{c}\right)^2$$

where t_o is the initiation time and a_o the initial crack length.

ie $$\left(\frac{ct_o}{a_o}\right)^2 = \frac{2G_1}{Eh}\left(\frac{c}{V}\right)^2 + \frac{2}{3} \tag{5}$$

2) Steady State Propagation

A constant static G_s is achieved for constant speed crack growth;

ie $$a = \dot{a}_o t \tag{6}$$

for which $\ddot{a} = 0$ and $\frac{\dot{a}t}{a} = 1$ and hence for propagation,

$$G_o = \frac{Eh}{2}\left(\frac{V}{\dot{a}_o}\right)^2 - \frac{Eh}{2}\left(\frac{V}{c}\right)^2$$

and $$\left(\frac{c}{\dot{a}_o}\right)^2 = \frac{2G_o}{Eh}\left(\frac{c}{V}\right)^2 + 1 \qquad (7)$$

Note that as $V \to \infty$, and $G_o \to 0$, $\dot{a}_o \to c$ and that for a finite initial crack length the boundary conditions of this solution are violated since at $t = t_o$

$$\left(\frac{ct_o}{a}\right)^2 = \frac{2G_o}{Eh}\left(\frac{c}{V}\right)^2 + 1$$

and thus from equation (5), $a \neq a_o$. Also $\dot{a} = 0$ at initiation and not $\dot{a}_o$ thus stimulating transients in the motion of a.

3) Transient Solution

The full equation of motion for constant G is somewhat intractable, but a useful solution is obtained by considering a small perturbation, p, from the steady state;

$$a = \dot{a}_o t + p \qquad (8)$$

substituting in equation (4) we have,

$$\frac{1}{b}\frac{dU_k}{da} = \frac{Eh}{2}\left(\frac{V}{c}\right)^2\left(1 + \frac{\ddot{p}t}{\dot{a}_o}\right)$$

and hence

$$G_o = \frac{Eh}{2}\left(\frac{V}{\dot{a}_o}\right)^2\left(1 - \frac{2p}{\dot{a}_o t}\right) - \frac{Eh}{2}\left(\frac{V}{c}\right)^2\left(1 + \frac{\ddot{p}t}{\dot{a}_o}\right)$$

ie $$\left(\frac{c}{\dot{a}_o}\right)^2 = \left[\frac{2G_o}{Eh}\left(\frac{c}{V}\right)^2 + 1\right] + \frac{1}{\dot{a}_o t}\left[2\left(\frac{c}{\dot{a}_o}\right)^2 p + \ddot{p}t^2\right] \qquad (9)$$

Thus for small perturbations the equation of motion for p is,

$$0 = \alpha p + \ddot{p}t^2 \qquad (10)$$

where $\alpha = 2\left(\frac{c}{\dot{a}_o}\right)^2 = 2\left[\frac{2G_o}{Eh}\left(\frac{c}{V}\right)^2 + 1\right]$

Equation (10) has a solution of the form;

$$p = const.\ t^{\frac{1}{2} \pm i\varepsilon}$$

where $\varepsilon = \frac{1}{2}\sqrt{4\alpha - 1} = \frac{1}{2}\sqrt{8\left(\frac{c}{\dot{a}_o}\right)^2 - 1}$ (11)

which has a real part of;

$$p = \left(\frac{t}{t_o}\right)^{\frac{1}{2}}\left[B_1 \sin\left(\varepsilon \ln\frac{t}{t_o}\right) + B_2 \cos\left(\varepsilon \ln\frac{t}{t_o}\right)\right] \qquad (12)$$

The constants B_1 and B_2 can be found from the mismatch in a and $\dot{a}$ at $t = t_o$ discussed previously;

i.e., at $t = t_o$, $\dot{p}_o = -\dot{a}_o$ and $p_o = a_o(1-\beta)$

where

$$\beta^2 = \left(\frac{\dot{a}_o t_o}{a_o}\right)^2 = \frac{\frac{2}{3} + \gamma\left(\frac{2G_o}{Eh}\right)\left(\frac{c}{V}\right)^2}{1 + \left(\frac{2G_o}{Eh}\right)\left(\frac{c}{V}\right)^2} = \gamma - \left(\gamma - \frac{2}{3}\right)\left(\frac{\dot{a}_o}{c}\right)^2$$

and $\varepsilon^2 = \frac{21\gamma - 16 + 3\beta^2}{12(\gamma - \beta^2)}$ with $\gamma = \frac{G_1}{G_o}$ the ratio of initiation to propagation toughness.

We have finally,

$$\left.\begin{aligned} \frac{a}{a_o} &= \beta\tau + \tau^{\frac{1}{2}}\left[(1-\beta)\cos X - \frac{(1+\beta)}{2\varepsilon}\sin X\right] \\ \frac{\dot{a}}{\dot{a}_o} &= 1 - \tau^{-\frac{1}{2}}\left[\cos X + \frac{1}{\beta}\left(\frac{(1+\beta)}{4\varepsilon} + (1-\beta)\varepsilon\right)\sin X\right] \end{aligned}\right\} \qquad (13)$$

where $\tau = \frac{t}{t_o}$ and $X = \varepsilon \ln \tau$.

The form of the perturbations is shown in fig 2 where $\frac{\dot{a}}{\dot{a}_o}$ is shown as a function of τ. For low crack speeds $\beta \to 1$ and $\varepsilon \to \infty$ giving very rapid oscillations between bounds of $\pm\tau^{-\frac{1}{2}}$ as shown. As the crack speed increases the frequency decreases as ε decreases and a typical curve for $\beta = 0.95$, $\varepsilon = 2{\cdot}6$, $\frac{\dot{a}_o}{c} = {\cdot}54$ is shown which illustrates the decreasing frequency with time. The upper bound as $V \to \infty$ or $G_o \to 0$ is also shown for which $\beta^2 = \frac{2}{3}$, $\varepsilon = 1{\cdot}32$, $\frac{\dot{a}_o}{c} = 1$. These oscillations result in oscillations in the crack growth which are manifest in variations from the steady state.

THE DOUBLE CANTILEVER BEAM DCB

A similar, though rather more complicated, analysis may be applied to the DCB specimen which is used in composites testing [4]. The equivalent solutions are

$$\beta^4 = \left[\frac{\frac{22}{37} + \gamma\frac{560}{111}\cdot\frac{G_o}{Eh}\left(\frac{c}{V}\right)^2}{1+\frac{560}{111}\cdot\frac{G_o}{Eh}\left(\frac{c}{V}\right)^2}\right] \quad \text{and} \quad \varepsilon^2 = \frac{573\gamma - 352 + 19\beta^4}{304\left(\gamma-\beta^4\right)} \tag{14}$$

The steady state solution here is not constant speed but $a = A\sqrt{t}$ where

$$\left(\frac{ch}{A^2}\right)^2 = \frac{8}{3}\frac{G_o}{Eh}\cdot\left(\frac{c}{V}\right)^2 + \frac{37}{70} \tag{15}$$

and using similar boundary conditions,

$$\frac{p}{a_o} = \left[(1-\beta)\cos X - \left(\frac{1+\beta}{4\varepsilon}\right)\sin X\right] \tag{16}$$

$$\frac{\dot{p}t_o}{a_o} = -\tau^{-\frac{3}{4}}\left[\cos X + \frac{1}{\beta}\left(\frac{(1+\beta)}{8\varepsilon} + 2\varepsilon(1-\beta)\right)\sin X\right] \tag{17}$$

Note that the velocity is scaled on that in the steady state at $t = t_o$, ie

$$\dot{a}_o = \frac{A}{2\sqrt{t_o}} = \frac{\beta a_o}{2t_o}$$

and that there are pronounced similarities in form with equations 13.

SOME EXPERIMENTAL RESULTS

Figure 3 shows crack growth data taken from a double torsion test on polyethylene [11]. A mean line corresponding to the steady state is shown and the oscillating variations predicted by the transient analysis are apparent. These are re-plotted in fig 4 as $\frac{p}{a_o}$ versus time and compared with those predicted from the analytical result using $\varepsilon = 8$ and $\beta \approx 1$ in this case. The general agreement is satisfactory both in form and magnitude, though for times above 0.7 ms there are crack arrests which limit crack growth. The analysis of data from these tests will be pursued further elsewhere [12].

The data shown in fig 3 is obtained from a conducting strip crack gauge and only measures crack length every 10 mm or so which limits the accuracy possible in the perturbation measurements. Fig 5 shows results obtained on a DCB specimen made from a carbon fibre-epoxy laminate, where the crack length measurements are obtained from a high speed camera, where readings can be taken every 5mm and a better defined curve is obtained [3]. Also shown is the steady state solution clearly indicating the crack perturbations. With this number of points it is possible to make some estimate of crack speed and this is shown in fig 6 together with the steady state result. The crack length perturbation data are shown in fig 7, together with the prediction of equation 16 with $\beta = 1{\cdot}13$ and $\varepsilon = 4{\cdot}5$ and the perturbation velocity data are compared with equation (17) in fig 8 for the same parameters. The fit in both cases is good and supports the general validity of the analysis.

CONCLUSIONS

The results show that the general method of using the static displacements to compute the kinetic energy, although not exact, yields useful results. Experimental systems function close to "steady state" conditions which are those which would pertain if the crack histories could commence at $a = 0$ at $t = 0$. Practically this is never possible since specimens must be pre-cracked and all cracks commence growth under conditions which are not in accordance with the steady state. This is mainly because a finite velocity is required at initiation, but in reality all cracks initiate at $\dot{a} = 0$. Arguments about crack being inertia-less bodies, such that finite initiation velocities occur, do not appear to be true in practice. This is borne out by the perturbation analysis which shows oscillating growth which is observed in practice.

In practical terms it seems that dynamic tests at fixed speeds, or slowly varying speeds as in the DCB are hard to achieve in practice. Indeed the analysis would imply that in real failures varying velocities are likely. The saving grace is that the notion of G_c being constant at these high rates seems to be a reasonable assumption and can be estimated. The analysis problem is one of dynamics rather than fracture, since the behaviour of rapid cracks is mostly governed by the interchange of strain and kinetic energies with that absorbed by fracture playing a minor rôle.

REFERENCES

1. Hashemi, S., Kinloch, A.J., and Williams, J.G. (1990). *Proc. R.. Soc. Lond.* A427, 173.
2. European Structural Integrity Society (ESIS) Protocol on determination of G_{IC} for Composite Laminates.
3. Blackman, B.R.K., Dear, J.P., Kinloch, A.J., MacGillivray, H., Wang, Y., Williams, J.G. and Yayla, P. (1995). *J. Mat. Sci.*, 5885.
4. Blackman, B.R.K., Kinloch, A.J., Wang, Y. and Williams, J.G. (1996). Acc. for pub. *J. Mat. Sci.*
5. Williams, J.G. (1994). *Eur. J. Mech.*, A/Solids 13, No 4 , suppl., 227.
6. Wang, Y., and Williams, J.G. (1994). *Composites* 25, No. 5, 323.
7. Williams, J.G. (1995) Dynamic Fracture Analysis of the DCB Specimen. *Proc. 1995 ASME/JSME Pressure Vessels and Piping Conference.*
8. Berry, J.P. (1960). *J. Mech. Phys.Solids,* 8, No 3, 194.
9. Berry, J.P. (1960). *J. Mech. Phys.Solids,* 8, No 3, 207.
10. Williams, J.G. (1993). *Strain Anal. for Engng. Design*, 28, No 4, 237.
11. Ritchie, S, (1996). The High Speed Double Torsion Test, PhD Thesis, London University.
12. Ritchie, S, Leevers P., Williams J.G. to be published.

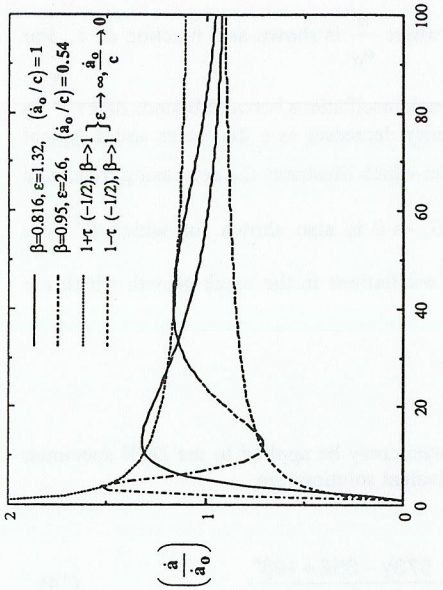

Figure 2. Variations of velocity with time for the parallel strip

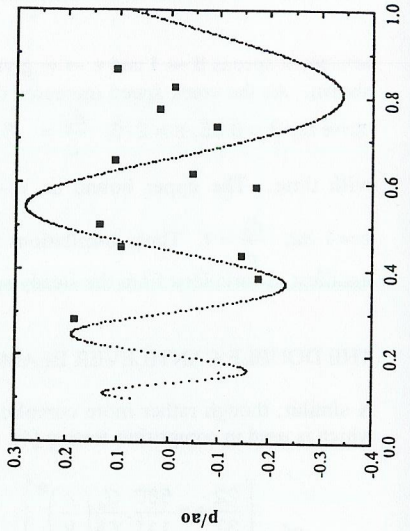

Figure 4 Perturbation versus time data

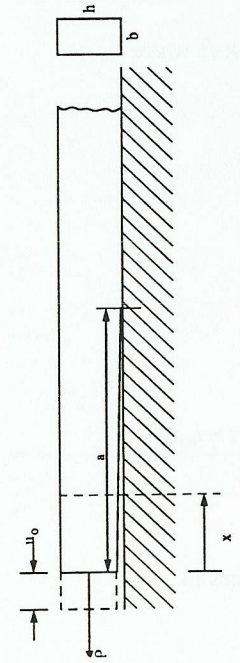

Figure 1. The axially loaded strip.

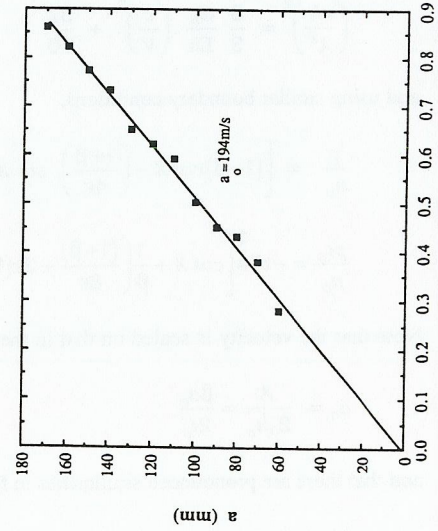

Figure 3. Crack length versus time data for a double torsion impact test on polyethylene

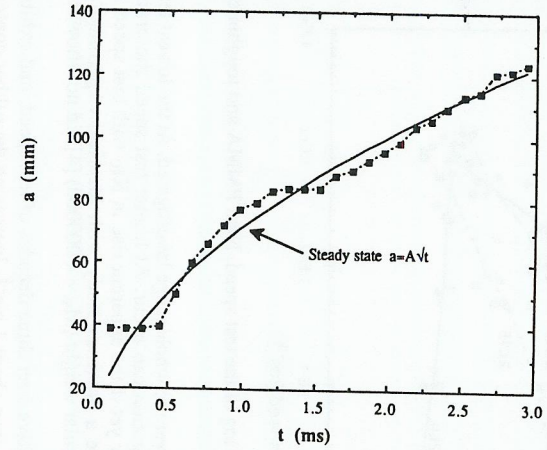

Figure 5. Crack length versus time data for a carbon fibre-epoxy laminate

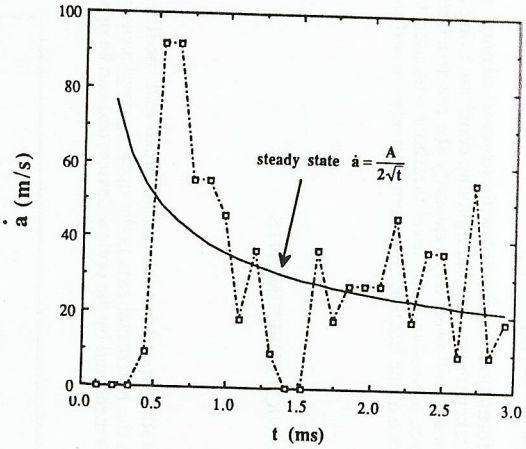

Figure 6. Crack speed versus time taken from figure 5

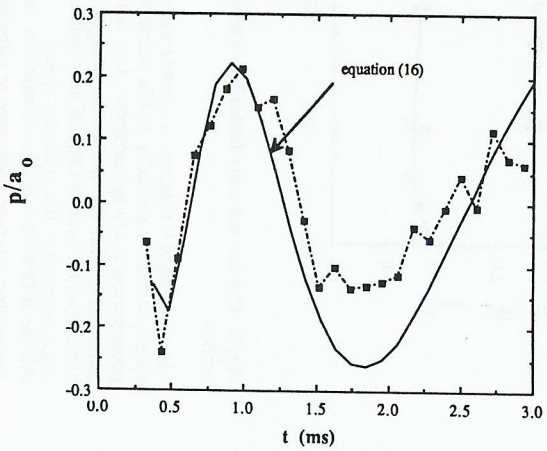

Figure 7. Crack length perturbation as a function of time. $\beta = 1.13$, $\varepsilon = 4.5$

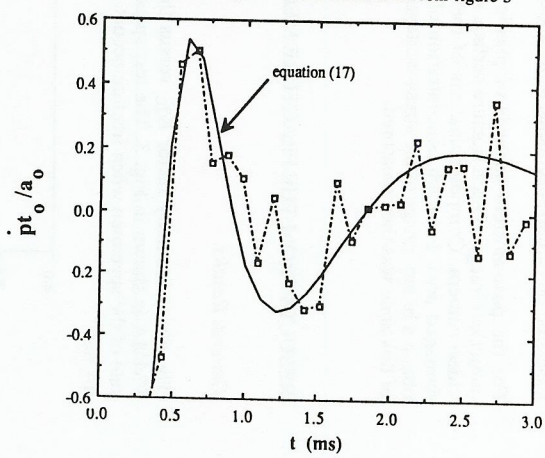

Figure 8. Crack velocity perturbation as a function of time. $\beta = 1.13$, $\varepsilon = 4.5$